RELATIONSHIPS BETWEEN BIOPHYSICAL PARAMETERS AND POLARIMETRIC AIRSAR DATA IN THE TROPICAL SAVANNAS OF NORTHERN AUSTRALIA

Authors:

Carl H. Menges <carl@gis.ntu.edu.au>
Faculty of Science, Northern Territory University, Darwin NT 0909, Australia
Anthony O'Grady <a_ogrady@bligh.ntu.edu.au>
Faculty of Science, Northern Territory University, Darwin NT 0909, Australia
and Waqar Ahmad <w_ahmad@banks.ntu.edu.au>
Faculty of Science, Northern Territory University, Darwin NT 0909, Australia

Abstract: This study attempts to identify the relationship between AirSAR backscatter and the biophysical parameters of five vegetation communities in the tropical savannas of northern Australia. The basal area, biomass, and leaf area index was measured for 29 sites coincident with image acquisition. Regression analysis of the data reveals that correlation coefficients are high only for averages of all data within the vegetation communities sampled. If all ground data sites are considered the correlation coefficients are relatively low, which is most likely attributable to the heterogeneity of this environment and the inherent error in geographic location determined by GPS. No polarization or frequency of the AirSAR data shows a consistent relationship with biophysical parameters.

1. Introduction

Tropical savannas are of great importance to tropical regions and are of global significance, due to the impact on the global carbon balance. These encompass almost all the coastal and subcoastal lands of Northern and Eastern Australia, north of the Tropic of Capricorn, covering more than one fifth of the continent (Lindsay 1996). Tropical savannas are a complex vegetation community, where grasses, shrubs and trees co-exist in dynamic equilibrium providing the natural resources for economic enterprises that contribute A$ 7.5 billion annually to the national economy. Much of this is in export income from the mining, tourism and grazing industries, and accounts for more than one fourth of Australia's export merchandise. Appropriate management to ensure ecologically sustainable development is essential if we are to prevent degradation of the resources that provide the base for these industries (Winter and Williams 1996, Lindsay 1996).

The use of Synthetic Aperture Radar (SAR) to map the forests and woodlands and to monitor the long term developments in these ecosystems is desirable because large area coverage can be achieved at regular intervals at relatively low cost. SAR is superior to optical remotely sensed data due to its ability to penetrate cloud cover, thus making resource monitoring during the wet season possible.

The relationship between polarimetric SAR backscatter and total above ground biomass has been investigated by many researchers for monospecific pine forests, coniferous forests, and mixed deciduous and coniferous forests in North America and Europe. Radar backscatter has been successfully employed to estimate biomass (Hussin et al. 1991; Wang et al. 1995; Miguel-Ayanz 1996; Rauste et al. 1994; Ranson et al. 1997; Ranson and Sun 1994; Harrell et al. 1997; Rignot et al. 1994a; Kasischke et al. 1994; Foody et al. 1997), to discriminate forest and grassland communities according to structural variation (Dobson et al 1992; Kasischke et al. 1997; Rignot et al. 1994b; Rignot et al. 1997; Saatchi et al. 1997; Harrell et al. 1997; Miguel-Ayanz 1996; Yanasse et al. 1997; Imhoff et al. 1997; Rosenqvist 1996), and to estimate leaf area (Steven and Jaggard 1996; Imhoff et al. 1997). The results indicate that the sensitivity of radar backscatter to variation in biomass varies with polarization and radar wavelength and is limited by a saturation level. The saturation level increases with wavelength and the HV polarization shows the greatest level of sensitivity conditions. Saturation level at L-HV has been placed as high as 300 tons per hectare (Kasischke et al. 1997). Moghaddam et al. (1994), however, reported that no unique relationship between radar backscatter and biomass exists for their study area. Similarly, only a weak relationship between backscatter and biomass was found for regenerating tropical rainforest in Brazil (Foody et al. 1997). The strength of the relationship was found to increase for ratios between the backscattering components HV and HH at L-Band. The L-HV / C-HV ratio, was found to be weakly correlated against expectations from previous research (Dobson et al. 1995; Ranson et al. 1995). These results were attributed to the mixture of species contributing to variability in canopy geometry as a more significant relationships could be achieved upon separation of the species. The study of correlations between radar backscatter and vegetation parameters is therefore not universal and must be established for specific environments or tree species.

A study conducted in the Northern Territory of Australia found that C-HV was highly correlated to leaf area index (LAI), and L-VV and P-VV to a normalized measure of biomass (surface area over volume) of branches and stems respectively (Imhoff et al. 1997). These results are contrary to other studies as the VV polarization is generally seen as being the least responsive to biomass variation. The correlation to LAI is also unique. The study was primarily aimed at the discrimination of three distinct vegetation communities across two well-defined boundaries. The correlation may, therefore, be at least partially attributable to changes in canopy geometry rather than vegetation parameters between the three communities.

This paper presents the results of an empirical evaluation of the sensitivity of radar scattering components to above ground biomass and LAI for the tropical savannas of northern Australia. Contrary to previous studies, all nine independent scattering components contained in the Stokes matrix for each wavelength have been included in the analysis. The ground data has been gathered at the time of radar data acquisition for 126 samples of five dominant vegetation communities ranging in LAI from 0.1 to 2.4 m^2 per m^2 and wet weight above ground biomass from 19 to 160 tons per hectare.

2. Study Area

The savannas of northern Australia occupy approximately 25% of the Australian continental landmass. Climate is monsoonal with more than 95% of the annual rainfall (average 1700 mm) falling in the summer months of October to April. While an annual monsoon is predictable the timing and onset of the monsoons varies between years (Taylor and Tulloch 1985). Maximum daily temperatures and evaporation rates remain high throughout the year, ranging from 35 ^{o}c in the wet season to 31 ^{o}c during the dry season (Hickey, 1985) and evaporation rates of about 6-8 mm per day (Hutley *et al.* 1999). Distinct rainfall, temperature and humidity variation within these periods have created a diverse assemblage of savanna vegetation in northern Australia. This varies from well vegetated areas to sparsely vegetated areas and the composition and structure appears to be governed to a large extent by soil water availability and to a lesser extent nutrient availability (Willams *et al.* 1996), with fire also being an important determinant of savanna structure (Andersen *et al.* 1998).

The current study was conducted in the Gunn Point region approximately 50 km east of Darwin (130^{0} $45^{'}$E, 12^{0} $30^{'}$ S) in the Northern Territory (Fig. 1).

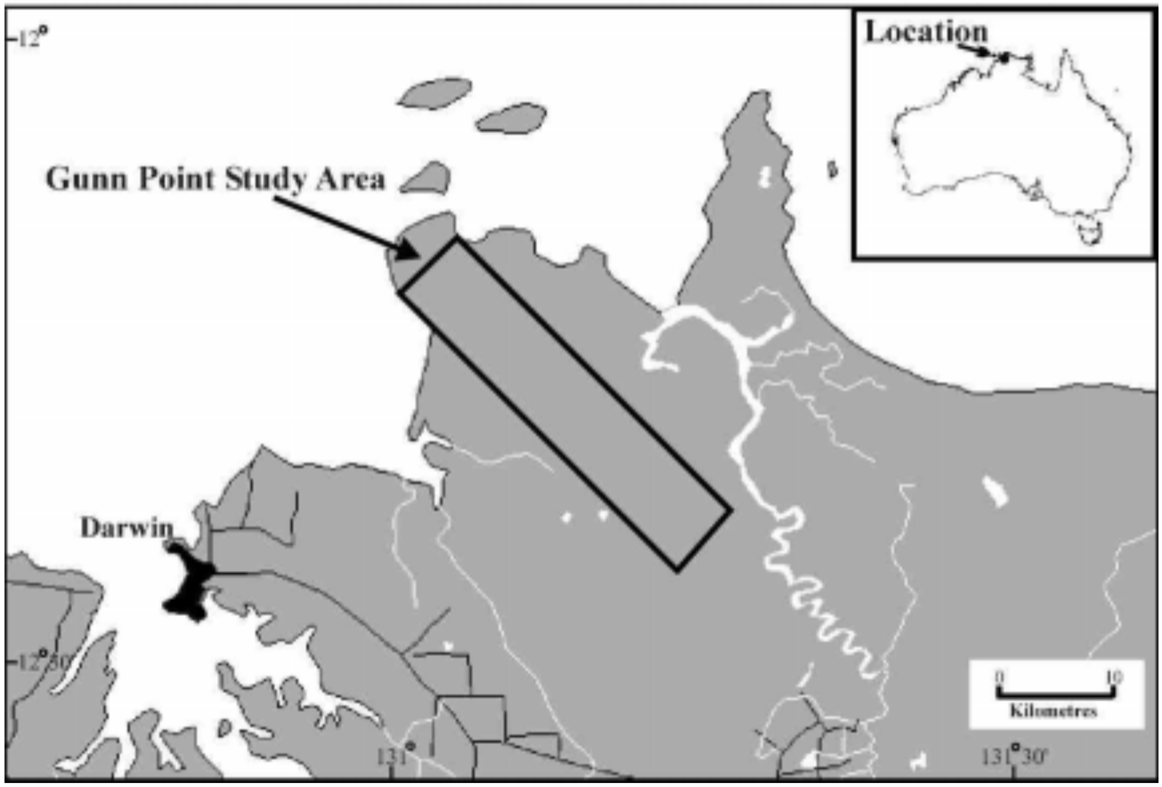

Figure 1. Location of the Study Area

The area was dominated by *E. miniata/E. tetrodonta* open forests, a dominant forest type north of the 1200mm isohyet. The area was chosen due to the availability of recently acquired digital and other ancillary data such as ground survey data, vegetation type and land system/units maps. The *E. miniata/E. tetrodonta* open forests form the matrix within which other important vegetation communities occur, ranging from wetlands to closed monsoon forests. Soils in the area are characterised by red and yellow sandy clay loams derived from highly weathered laterites of the Koolpinyah plateau (Bowman and Wrightman 1986). The topography of the study area is flat with no significant variation in elevation.

3. Data and Methodology

3.1 Ground Data Collection

Species composition, leaf area index, canopy cover and basal area were surveyed in dominant vegetation communities of the Gunn Point region. Communities and sites were identified using a 1:100000 vegetation map of the area (Ahmad et al. 1997). Sampling was restricted to a 10 km strip corresponding to the flight path of the radar.

Vegetation communities were sampled using a random stratification sampling technique. Communities sampled are shown in table 1. Five locations were chosen within each vegetation type and species and structural data were collected in each of three 20 x 20 m plots at each location. The location of each plot was recorded using a hand held GPS at the center of each plot. Each tree within a plot was identified to species level and the diameter at 1.3 m (DBH) and leaf area were recorded. Leaf area of each tree was estimated via the 'Adelaide technique' (Andrew *et al*. 1979). The technique is described in detail by O'Grady *et al.* (2000), but involves counting the number of leaf modules on each tree. Reference modules for each species were collected and the leaf area of each module determined using planimetery (Delta T leaf area meter, Cambridge UK.). Leaf area index of the plot was then estimated by summing the leaf area of all trees and dividing by the area of the plot (400 m^2). Canopy cover in each plot was estimated using a spherical densiometer (Lemmon 1957) and canopy cover was estimated at three random location within each plot. The above ground wet biomass was calculated using the allometric equation: Biomass $= 1.0455 (DBH)^2 - 5.1779 (DBH) + 8.6881$ (r^2=0.9058)

Table 1. Vegetation Communities Sampled During November 1996. Five Locations were Selected for each Community Type and Leaf Area Index, Canopy Cover and Basal Area were Recorded in each of Three 20*20m Plots at each Location.

Community Type
E. tetrodonta forest.
E. tetrodonta/E. miniata open forest
E. bleeseri/E. miniata woodland
E.bleeseri/E. miniata/E. tetrodonta woodland
G. pteridifolia/P. spiralis open woodland
M. cajuputi/A. symphocarpus forest

3.2 Data Processing

The JPL AIRSAR system was flown over the study site on board a DC-8 on the 23rd of November 1996. The AIRSAR acquired backscatter data at C-band (wavelength=5.6 cm, frequency=5.3 Ghz), L-band (23.9 cm, 1.25 Ghz) and P-band (67.0 cm, 0.44 Ghz) in four transmit / receive polarisations (HH, VV, HV, VH). Local time of data acquisition was 11.00 am under dry weather conditions with some cloud present. The AIRSAR data were processed as a 60km strip product by JPL's Radar Data Centre using version 6.1 of the integrated processor, and supplied in 18 look compressed Stokes matrix format. The look angle ranges from 22.6 degrees to 61.7 degrees in the range direction.

The Stokes Matrix for polarimetric SAR data is a 4x4 matrix (van Zyl and Ulaby, 1990). Due to the assumption of symmetry (i.e. $S_{hv} = S_{vh}$) and averaging as part of the multi-look processing a maximum of nine independent numbers need to be stored for each image pixel (Zebker and van Zyl, 1991). The compressed Stokes Matrix as processed by

JPL's Radar Data Centre, therefore, contains 10 bytes of information per pixel, with two bytes being used to store the total power.

Nine independent elements describing the scattering behaviour can be extracted for each frequency (see table 2). Five of these components that contain valuable information (Baker et al. 1994) are considered here. The three bands containing the magnitude of the backscatter at HH, VV and HV polarization as well as the real and imaginary component of the co-polarized backscatter. The latter two components can be used to compute the HH-VV phase difference and the correlation coefficient.

Table 2. Elements of the Scattering Matrix Extracted from the Compressed Stokes Matrix Format

Sacttering element	Description
$<S_{HH}S_{HH}^{*}>$	Magnitude of HH return
$<S_{VV}S_{VV}^{*}>$	Magnitude of VV return
$<S_{HV}S_{HV}^{*}>$	Magnitude of HV return
$Re<S_{HH}S_{VV}^{*}>$	Real part of HH-VV copolarised return
$Im<S_{HH}S_{VV}^{*}>$	Imaginary part of HH-VV copolarised return
$Re<S_{HH}S_{HV}^{*}>$	Real part of HH-HV crosspolarised return
$Im<S_{HH}S_{HV}^{*}>$	Imaginary part of HH-HV crosspolarised return
$Re<S_{HV}S_{VV}^{*}>$	Real part of HV-VV crosspolarised return
$Im<S_{HV}S_{VV}^{*}>$	Imaginary part of HV-VV crosspolarised return

The SAR data was corrected to minimise incidence angle related backscatter variation. The co-polarised returns were corrected for incidence angle using the LUT method. This method, is based on the correction technique outlined in Menges et al. (1999a, 1998). Here, the range line at the nominal incidence angle, is used as a look up table to match values of other rangelines. The AIRSAR data are used as well as the numerically sorted frequency distribution data of the rangelines generated in the previous stage. The procedure operates on a pixel by pixel basis on the AIRSAR data. The backscatter value of each pixel is noted together with its range distance. This backscatter value is searched for in the frequency distribution look up table at the same range line. In the numerically sorted frequency distribution look up table the row number at which the value is found indicates the percentile value of the cumulative frequency of the value's occurrence for that particular range line. Now the value associated with this cumulative frequency in the norm line can be determined and written to the "corrected" image.

The magnitude components of the SAR data set were corrected for the effect of variation in incidence angle using the slope of the linear regression determined for each line of constant incidence angle versus the norm line (Menges et al. 1999b). The values within the lines are numerically sorted for this purpose and the slope of the regression applied to the individual lines of data.

A 3 x3 averaging filter was applied to all channels to reduce the effective resolution of the data approximating the optimal resolution for the detection of these ecological units (Menges et al. 1999c) and to reduce the speckle. The data is supplied by JPL as an 18-look average. Calculation of the Equivalent Number of Looks (ENL) as the ratio of the square of the mean divided by the variance for a homogeneous distributed target resulted in a value of 6.3 for the raw data. The ENL for the mean filtered intensity data equals 26.4 using the same target.

After conversion to ground range format the data was registered to 1:50,000 scale topographic maps with an RMS error of less than 10 metres and resampled using bilinear interpolation to reassign pixel values. Extraction of data values was performed according to GPS readings recorded in the field by identification of the pixel at that location and calculating the average over a three by three neighbourhood.

4. Results and Discussion

Leaf area index, basal area and canopy cover were surveyed in a number of vegetation communities in the Gunn Point region. Mean LAI, basal area and canopy cover for each of the sampled communities is shown in table 3. DBH was an excellent predictor of tree leaf area; leaf area=$0.12(DBH)^2+0.32(DBH)+155$,$r^2=0.87$ (figure 2, from O'Grady *et al.* submitted). Leaf area index of a stand can be approximated from basal area of that stand using the straight line relationship LAI = 0.11(BA)+0.21, although there was considerable variation in this relationship ($r^2 = 0.49$).

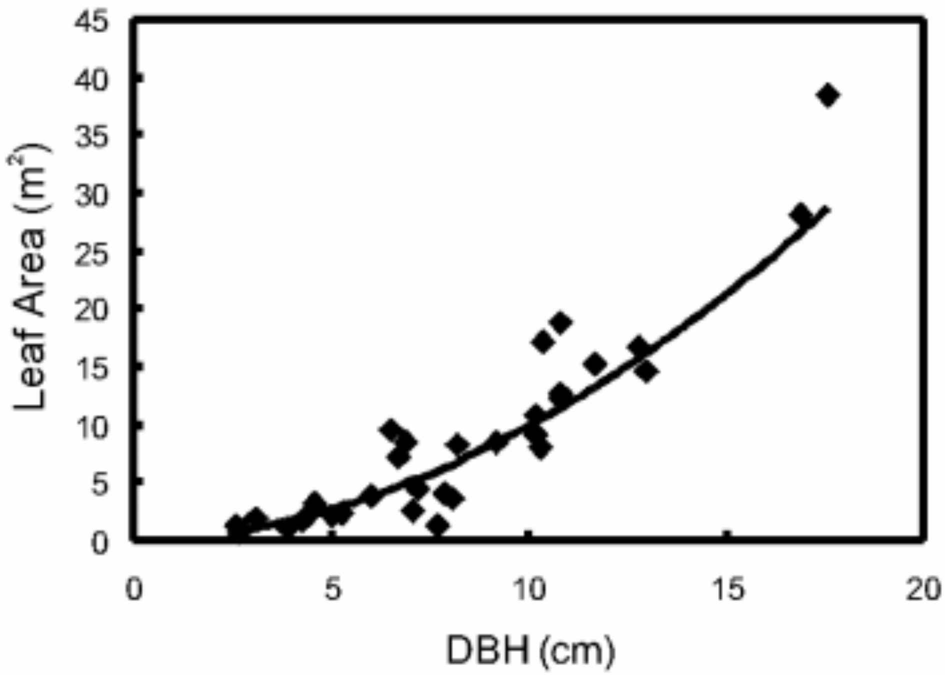

Figure 2. Allometric Relationship Between DBH (cm) and Leaf Area (m^2). A Second Order Polynomial of the Form $y=0.12x^2+0.32x+1.55$, $r^2=0.87$ Best Describes the Relation Between DBH and Leaf Area for Harvested Trees (From O'Grady *et al.* 2000).

The poor correlation between LAI and basal area may reflect the time of year that sampling was conducted. O'Grady *et al*. (2000) showed that the strength of this relationship varied seasonally and reflected changes in phenology and the impact of fire. November is a transitional period characterised by considerable leaf flushing in response to intermittent rainfall events (Myers *et al.* 1998) and declining atmospheric vapor pressure deficits (Williams *et al.* 1997)

The regression analysis of SAR data against biomass (table 4) and LAI (table 5) was initially conducted on the values derived for each of the 50x50m sample sites. The values represented are an average of the result for three 20x20m plots sampled within the boundaries of the sample site. The highest correlation to biomass is found for the HV and HH polarisations at L and P Band in accordance with numerous other studies (see Kasischke et al. 1997). A crossplot of these relationships is shown in figures 3 and 4. The relatively low correlation coefficients do not appear to be a result of a saturation effect, as there is significant variability throughout the range of values. A similarly weak correlation between backscatter components and biomass was reported by research on tropical rainforest in Brazil (Foody et al. 1997) and research by Dobson et al. (1995) and Ranson et al. (1995).

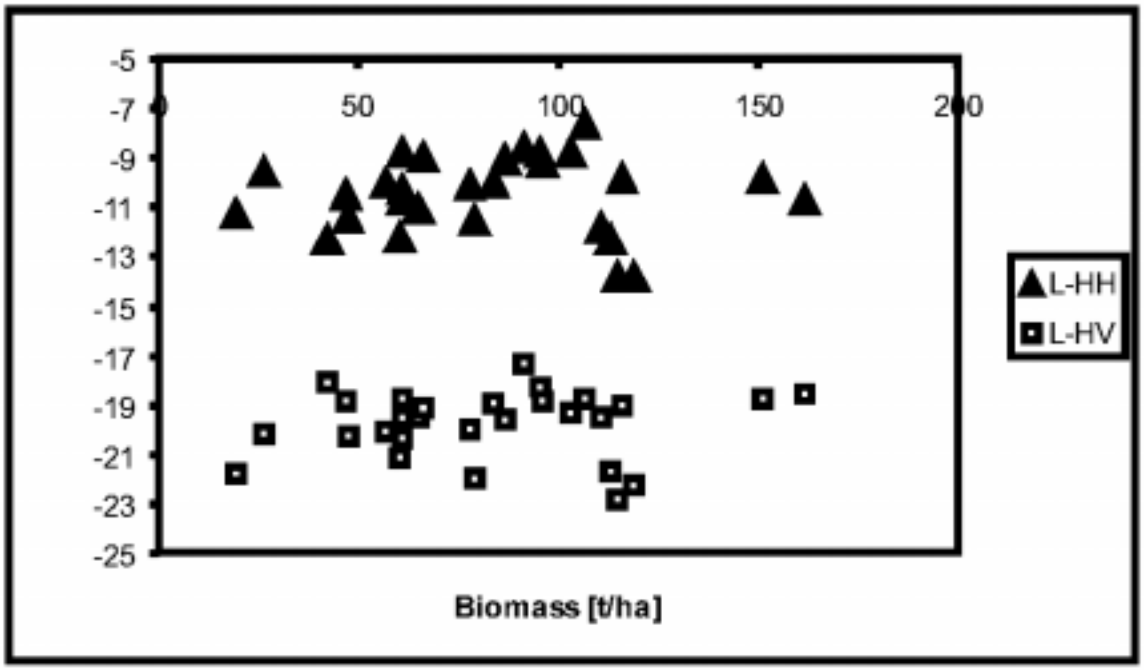

Figure 3. Crossplot of Biomass Versus L Band Backscatter at HH and HV Polarization.

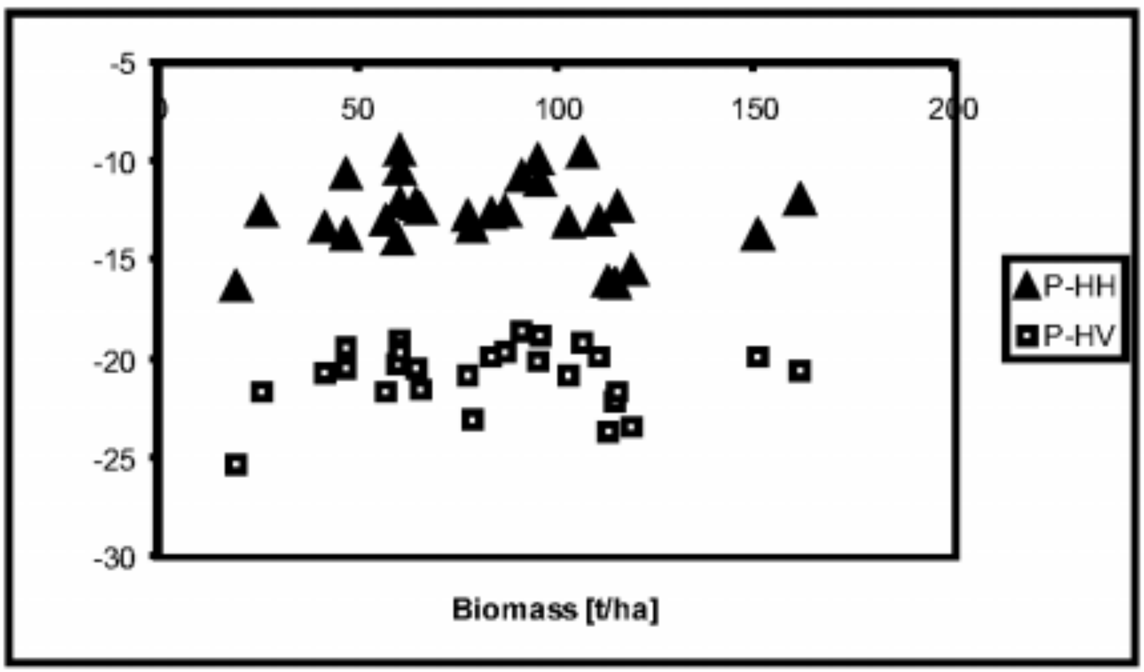

Figure 4. Crossplot of Biomass Versus P Band Backscatter at HH and HV Polarization.

Table 3. LAI, Basal Area and Canopy Cover for Vegetation Communities of the Gunn Point Region, November 1996. Data Represent the Mean Community Values Determined from Three Plots at each of 5 Locations within each Community Type.

Community	LAI	Basal area [m^2 ha^{-1}]	Canopy Cover [%]
E. tetrodonta forest	1.56	12.79	67.6
E. tetrodonta/E. miniata open forest	1.67	9.11	60.08
E. bleeseri/E. miniata woodland	1.13	8.35	67.33
E. bleeseri/E. miniata/E. tetrodonta woodland	0.92	6.77	41.46
M. cajuputi/A. symphocarpus forest	1.67	14.36	70.71
G. pteridifolia/P. spiralis open woodland	0.42	5.78	21.16

When the regression analysis is performed using the averages of the biomass and SAR data for all sites within each vegetation community the correlation improves significantly. As shown in table 4, the HV polarization at L and P Band are still highly correlated. However, other channels, C $<S_{HH}S_{HH}^*>$, C $<S_{VV}S_{VV}^*>$, L $<S_{VV}S_{VV}^*>$, P Re$<S_{HH}S_{VV}^*>$, also emerge as having a statistically significant (at a 95% confidence level) correlation to biomass.

Table 4. Correlation Coefficients for the Linear Regression of SAR Variables Against Biomass.

	Site Data	Community Averages	Eucalypt Woodlands	Eucalypt Open Forest	Melaleuca Forest
C $<S_{HH}S_{HH}^*>$	0.33	0.98	-0.27	0.34	0.30
C $<S_{VV}S_{VV}^*>$	0.36	0.91	-0.06	0.27	0.40
C $<S_{HV}S_{HV}^*>$	0.38	0.86	-0.09	0.31	0.38
L $<S_{HH}S_{HH}^*>$	0.44	0.97	0.32	0.64	0.06
L $<S_{VV}S_{VV}^*>$	0.39	0.94	0.82	0.48	-0.20
L $<S_{HV}S_{HV}^*>$	0.50	0.92	0.50	0.37	0.45
P $<S_{HH}S_{HH}^*>$	0.54	0.95	0.74	0.32	0.54
P $<S_{VV}S_{VV}^*>$	0.22	0.71	0.04	0.49	-0.22
P $<S_{HV}S_{HV}^*>$	0.59	0.94	0.82	0.35	0.44
C Re$<S_{HH}S_{VV}^*>$	0.14	0.86	0.10	0.28	-0.39
C Im$<S_{HH}S_{VV}^*>$	-0.03	-0.05	0.09	-0.17	0.67
L Re$<S_{HH}S_{VV}^*>$	-0.20	-0.65	-0.26	0.06	-0.57
L Im$<S_{HH}S_{VV}^*>$	-0.25	-0.79	0.03	-0.46	0.54
P Re$<S_{HH}S_{VV}^*>$	0.34	0.95	0.21	0.56	-0.23
P Im$<S_{HH}S_{VV}^*>$	-0.37	-0.05	-0.45	-0.32	-0.64

Table 5. Correlation Coefficients for the Linear Regression of SAR Variables Against Leaf Area Index.

	Site Data	Community Averages	Eucalypt Woodlands	Eucalypt Open Forest	Melaleuca Forest
C $<S_{HH}S_{HH}^{*}>$	0.37	0.84	-0.19	-0.02	0.80
C $<S_{VV}S_{VV}^{*}>$	0.41	0.67	-0.08	0.42	0.85
C $<S_{HV}S_{HV}^{*}>$	0.37	0.56	-0.20	0.47	0.86
L $<S_{HH}S_{HH}^{*}>$	0.60	0.88	0.31	0.58	0.50
L $<S_{VV}S_{VV}^{*}>$	0.60	0.71	0.67	0.58	0.42
L $<S_{HV}S_{HV}^{*}>$	0.57	0.68	0.25	0.72	0.76
P $<S_{HH}S_{HH}^{*}>$	0.60	0.91	0.67	0.27	0.94
P $<S_{VV}S_{VV}^{*}>$	0.35	0.39	-0.11	0.58	0.20
P $<S_{HV}S_{HV}^{*}>$	0.68	0.92	0.76	0.52	0.47
C $Re<S_{HH}S_{VV}^{*}>$	0.40	0.82	0.13	0.68	0.23
C $Im<S_{HH}S_{VV}^{*}>$	-0.05	-0.20	0.16	0.22	0.75
L $Re<S_{HH}S_{VV}^{*}>$	-0.47	-0.86	-0.22	-0.39	0.05
L $Im<S_{HH}S_{VV}^{*}>$	-0.49	-0.88	0.11	-0.53	-0.05
P $Re<S_{HH}S_{VV}^{*}>$	0.53	0.79	0.17	0.76	0.30
P $Im<S_{HH}S_{VV}^{*}>$	-0.27	0.03	-0.58	0.00	-0.93

The correlation coefficients between site averages and SAR data after a stratification of vegetation communities did not yield improved results. Both the channels for which a significant relationship exists and the strength of the relationship do not agree with results for all samples or those for the averages between communities. The Eucalypt woodlands.

Regression analysis of LAI versus SAR data show slightly better results (table 5). The correlation coefficients for the site data are slightly higher than those for biomass at L Band for all polarisations and at P Band for HH and HV polarization. When community averages are used, only the P Band has a significant relationship at HH and HV polarisations. The HV polarization at P Band also has the highest correlation coefficient for the Eucalypt woodland communities and a weak relationship with the other two communities shown. For the Melaleuca community, the C Band shows a significant relationship, as well as P HH and the imaginary part of the co-polarised return at P Band. These results are unexpected as the longer wavelength interact primarily with the larger structural components of the vegetation rather than the tree canopy or leaves. The existence of a strong relationship between DBH and LAI may provide an explanation. Structurally, there is a difference between a large number of small stems and a few large stems which may result in the same amount of basal area or biomass. This structural difference is reflected in the SAR data (Imhoff 1995).

The weak correlation between backscatter and individual sites was most likely due to the heterogeneity of the environment. The accuracy of a hand held GPS is generally within 40m. An uncertainty of the geographic location of the plot by this amount, however, can make a large difference. Three 20x20m plots sampled within the same 50x50m area of one of the selected sites for *E. bleeseri/E. miniata* woodland were measured with a biomass of 24, 59, and 112 tons per hectare respectively. The minimum, maximum, and range of the backscatter intensities occurring in a 50 metre area surrounding the GPS location of these plots are shown in table 8. Also shown is the summary of the backscatter intensities for all the plots available. For the HV polarization the variation in the 50 metre area is 55% at L-Band and 56% at P-Band relative to the range found for all plots. This large variability observed over a small area, well within the accuracy of the GPS error, is likely to introduce large errors into the assessment of correlation between field and SAR data. Figure 5 visually demonstrates the location of this 50x50m site in a subset of the AirSAR data and a zoom of the pixel neighbourhood.

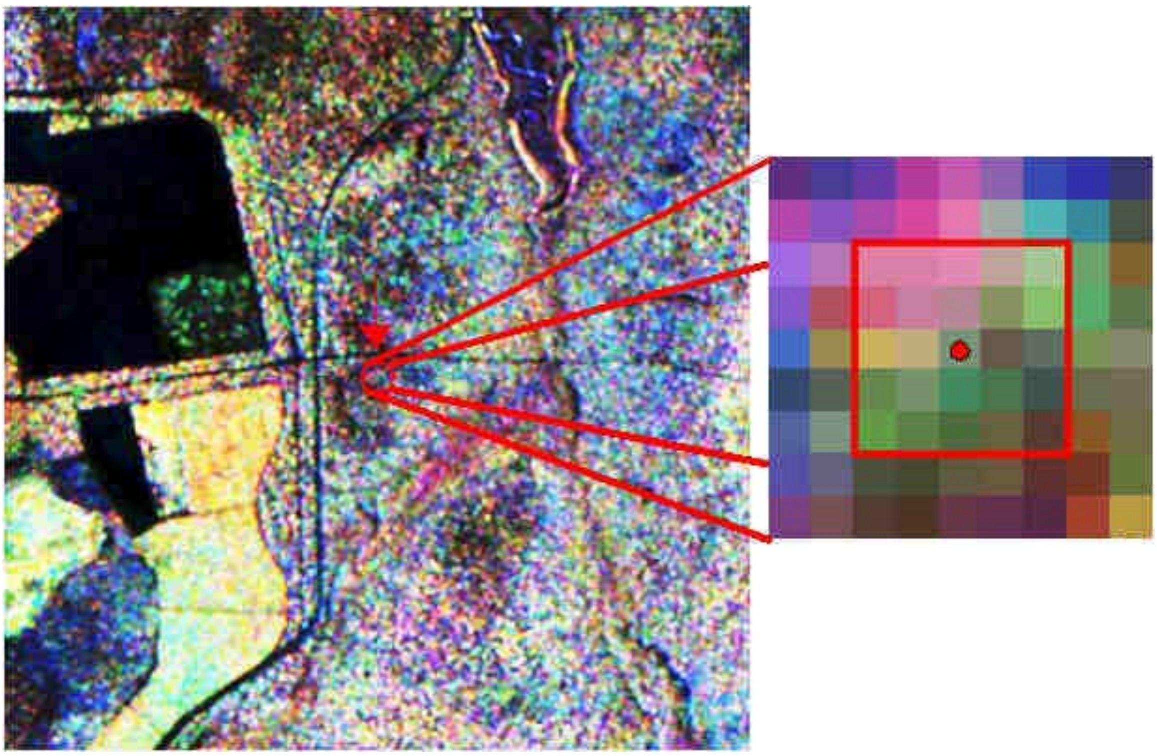

Figure 5. Colour Composite of AirSAR Data (P-HH, L-HH, and C-HH as RGB) of a Subset of the Study Area. A Zoom to the Centre of a 50x50m Ground Truth Site is Provided to Demonstrate the Heterogeneity of this Environment.

While the example provided showed the largest variability, it demonstrates that the conclusions that can be drawn from the analysis are limited. The presence of such a large error may cause an existing correlation to be obscured and increase the probability of a 'chance' correlation to occur. Either a very large number of sites is required to reduce this error, or more accurate locational information.

Table 8. The Variation in Backscatter Intensities for a Neighbourhood of 5x5 Pixels in Relation to that Observed for All Plots.

	Summary of backscatter for 5x5 neigbourhood			Summary of backscatter for all plots			Range relative to all
Band	Min	Max	Range	Min	Max	Range	plots [%]

C $\langle S_{HH}S_{HH}^{*}\rangle$	0.125	0.205	0.079	0.037	0.238	0.200	40
C $\langle S_{VV}S_{VV}^{*}\rangle$	0.100	0.154	0.054	0.007	0.177	0.170	32
C $\langle S_{HV}S_{HV}^{*}\rangle$	0.025	0.034	0.009	-0.004	0.048	0.052	17
C Re$\langle S_{HH}S_{VV}^{*}\rangle$	0.071	0.134	0.062	-0.049	0.069	0.118	53
C Im$\langle S_{HH}S_{VV}^{*}\rangle$	0.032	0.066	0.034	-0.049	0.022	0.071	48
L $\langle S_{HH}S_{HH}^{*}\rangle$	0.008	0.017	0.009	0.000	0.157	0.157	6
L $\langle S_{VV}S_{VV}^{*}\rangle$	0.032	0.077	0.045	0.000	0.089	0.089	51
L $\langle S_{HV}S_{HV}^{*}\rangle$	0.036	0.066	0.030	-0.027	0.027	0.054	55
L Re$\langle S_{HH}S_{VV}^{*}\rangle$	0.005	0.011	0.007	-0.055	0.026	0.080	8
L Im$\langle S_{HH}S_{VV}^{*}\rangle$	0.018	0.043	0.025	-0.055	0.003	0.058	44
P $\langle S_{HH}S_{HH}^{*}\rangle$	-0.015	0.031	0.046	0.000	0.124	0.124	37
P $\langle S_{VV}S_{VV}^{*}\rangle$	-0.005	0.020	0.025	0.000	0.172	0.172	14
P $\langle S_{HV}S_{HV}^{*}\rangle$	-0.018	0.000	0.018	-0.004	0.027	0.031	57
P Re$\langle S_{HH}S_{VV}^{*}\rangle$	0.003	0.022	0.020	-0.028	0.067	0.095	21
P Im$\langle S_{HH}S_{VV}^{*}\rangle$	-0.011	0.014	0.025	-0.028	0.013	0.041	61

5. Conclusion

This study confirmed that SAR data does not provide a universal tool for estimating biophysical parameters. The existence and strength of relationships are dependent on the vegetation community under investigation. For the study site in the tropical savannas of northern Australia, there is no single SAR parameter that can be shown to have a consistently strong relationship to the biomass or LAI of the vegetation communities present. The results of this study must be considered with caution because of the natural heterogeneity of this landscape, which makes the analysis difficult as small locational errors can distort the outcomes significantly. This is of greatest relevance to the results of the individual plots observed. After averaging of both ground and SAR data to a single value for each of the five vegetation communities, the correlation is significantly improved but reliability diminished through the reduction in data points. Further research is required into this relationship using a differential GPS system to reduce the locational error.

6. Acknowledgments

The authors would like to acknowledge the financial assistance of the Cooperative Research Centre for the Sustainable Development of Tropical Savannas.

7. References

Ahmad, W., O'Grady, A. P., Pfitzner, K., and Hill, G. J. E., (1997), Use of multispectral scanner data for the identification and mapping of tropical forests of northern Australia, in *Forests at the Limit: Environmental Constraints on Forest Function. International Union of Forest Research Organistaions Workshop*, Skukuza, Kruger National Park, South Africa.

Andersen A.N., R.W. Braithwaite, G.D. Cook, L.K. Corbett, R.J. Williams, M.M. Douglas, A.M. Gill, S.A. Setterfield and W.J. Muller (1998). Fire research for conservation management in tropical savannas: Introducing the Kalpalga fire experiment. *Australian Journal of Ecology,* 23, 95-110.

Andrew M.H., Noble I.R. and Lange R.T. (1979). A non-desructive method for estimating the weight of foliage on shrubs. *Australian Rangelands Journal,* 1: 225-231.

Bowman D.M.J.S. and G.M. Wrightman (1985). Small scale vegetation pattern associated with a deeply incised gully, Gunn Point, northern Australia. *Proceedings of the Royal Society of Queensland,* 96, 63-73.

Dobson, M. C., Ulaby, F. T., LeToan, T., Beaudoin, A., Kasischke, E. S., and Christensen, N., (1992), Dependence of Radar Backscatter on Coniferous Forest Biomass., *IEEE Transactions on Geoscience and Remote Sensing*, 30: 412-416.

Foody, G. M., Green, R. M., Lucas, R. M., Curran, P. J., Honzak, M., and Amaral, I. D., (1997), Observations on the Relationship Between SIR-C Radar Backscatter and the Biomass of Regenerating tropical forests, *International Journal of Remote Sensing*, 18: 687-694.

Harrell, P. A., Kasischke, E. S., Bourgeau_Chavez, L. L., Haney, E. M., and Christensen Jr., N. L., (1997), Evaluation of Approaches to Estimating Aboveground Biomass in Southern Pine Forests Using SIR-C Data, *Remote Sensing of Environment*, 59: 223-233.

Hutley L.B., A.P. O'Grady and D.Eamus (2000). Daily and seasonal patterns of evapotranspiration from eucalypt open-forest savanna of tropical northern Australia. *Functional Ecology,* (submitted).

Hussin, Y. A., Reich, R. M., and Hoffer, R. M., (1991), Estimating Slash Pine Biomass Using Radar Backscatter, *IEEE Transactions on Geoscience and Remote Sensing*, 29: 427-431.

Imhoff, M. L., Sisk, T. D., Milne, A., Morgan, G., and Orr, T., (1997), Remotely Sensed Indicators of Habitat Heterogeneity: Use of Synthetic Aperture Radar in Mapping Vegetation Structure and Bird Habitat, *Remote Sensing of Environment*, 60: 217-227.

Kasischke, E. S., Bourgeau, L. L., Christensen, J. N. L., and Haney, E. (1994). Observations on the Sensitivity of ERS-1 SAR Image Intensity to Changes in Aboveground Biomass in Young Loblolly Pine Forests, *International Journal of Remote Sensing*, 15: 3-16.

Kasischke, E. S., Melack, J. M., and Dobson, M. C., (1997), The Use of Imaging Radars for Ecological Applications - A Review, *Remote Sensing of Environment*, 59: 141-156.

Lemmon P.E. (1957). A new instrument for measuring overstorey density. *Journal of forestry*, 55: 667-668.

Luckman, A. J., (1997), Exploratory Study of the Relationship Between Tropical Forest Regeneration Stages and SIR-C L and C Data, *Remote Sensing of Environment*, 59: 180-190.

Menges, C., Crerar, J., Ahmad, W., and Hill, G. J. E., (1998), A Method for Estimating the Effect of Variation in Local Incidence Angle on AirSAR Data, in *9th*

Australasian Remote sensing and Photogrammetry Conference, Sydney, Australia, (Sydney: Causal Productions), 20-24th July ,CDRom, #145.
Menges, C., van Zyl, J. J., Hill, G. J. E., and Ahmad, W., (1999a), A Procedure for the Correction of the Effect of Variation in Local Incidence Angle on AIRSAR Data, *International Journal of Remote Sensing*: (submitted).
Menges, C., Hill, G. J. E., Ahmad, W., and van Zyl, J. J., (1999b), An Evaluation of Three Alternative Procedures for the Correction of the Effect of Variation in Local Incidence Angle on AirSAR Data, *Photogrammetric Engineering & Remote Sensing*: (submitted).
Menges, C., Hill, G. J. E., and Ahmad, W., (1999c), Use of Airborne Video Data for the Characterisation of Tropical Savannas in Northern Australia: The Optimal Spatial Resolution for Remote Sensing Applications, *International Journal of Remote Sensing*: (submitted).
Miguel-Ayanz, J. S., (1996), Synergy of Optical and Polarimetric Microwave Data for Forest Resource Assessment, *International Journal of Remote Sensing*, 17: 3647-3663.
Moghaddam, M., Durden, S., and Zebker, H., (1994), Radra Measurement of Forested Areas during OTTER, *Remote Sensing of Environment*, 47: 154-166.
Myers B.A., R.J. Williams, I. Fordyce, G.A. Duff and D. Eamus (1998). Does irrigation affect leaf phenology in deciduous and evergreen trees of the savannas of northern Australia. *Australian Journal of Ecology,* 23: 329-339.
O'Grady A.P., X.Chen, D. Eamus and L.B. Hutley (2000). Composition, structure, leaf area index and standing biomass of a eucalypt open forest near Darwin in the Northern Territory. *Australian Journal of Botany,* (in print).
Oliver, C. and Quegan, S. (Eds)(1997), *Understanding Synthetic Aperture Radar Images*: Artech House, London, UK.
Ranson, K. J. and Sun, G., (1994a), Mapping Biomass of a Northern Forest Using Multifrequency SAR Data, *IEEE Transactions on Geoscience and Remote Sensing*, 32: 388-396.
Ranson, K. J. and Sun, G., (1994b), Northern Forest Classification Using Temporal Multifrequency and Multipolarimetric SAR Images, *Remote Sensing of Environment*, 47: 142-153.
Ranson, K. J. and Sun, G., (1997), An Evaluation of AIRSAR and SIR-C/X-SAR Images for Mapping Northern Forest Attributes in Maine, USA, *Remote Sensing of Environment*, 59: 203-222.
Rauste, Y., Haeme, T., Pulliainen, J., Heiska, K., and Hallikainen, M., (1994), Radar-Based Forest Biomass Estimation, *International Journal of Remote Sensing*, 15: 2797-2808.
Rignot, E., Way, J., Williams, C., and Viereck, L., (1994a), Radar Estimates of Aboveground Biomass in Boreal Forests of Interior Alaska, *IEEE Transactions on Geoscience and Remote Sensing*, 32: 1117-1124.

Rignot, E. J. M., Williams, C. L., Way, J., and Viereck, L. A., (1994b), Mapping of Forest Types in Alaskan Boreal Forests Using SAR Imagery, *IEEE Transactions on Geoscience and Remote Sensing*, 32: 1051-1059.

Rignot, E., Salas, W. A., and Skole, D. L., (1997), Mapping Deforestation and Secondary Growth in Rondonia, Brazil, Using Imaging Radar and Thematic Mapper Data, *Remote Sensing of Environment*, 59: 167-179.

Rosenqvist, A., (1996), Evaluation of JERS-1, ERS-1 and Almaz SAR Backscatter for Rubber and Oil Palm Stands in West Malaysia, *International Journal of Remote Sensing*, 17: 3219-3231.

Saatchi, S. S., Soares, J. V., and Alves, D. S., (1997), Mapping Deforestation and Land Use in Amazon Rainforest by Using SIR-C Imagery, *Remote Sensing of Environment*, 59: 191-202.

Taylor J.A. and D. Tulloch. (1985). Rainfall in the wet-dry tropics: extreme events at Darwin and similarities between years during the period 1870-1983 inclusive. *Australian Journal of Ecology,* 10: 281-295.

van Zyl, J.J. and Ulaby, F.T., (1990), Scattering Matrix Representations for Simple Targets, Radar Polarimetry for Geoscience Applications, Artech House, Norwood, MA, pp.17-52.

Wang, Y., Davis, F. W., Melack, J. M., Kasischke, E. S.,, and Christensen, J. N. L., (1995), The Effects of Changes in Forest Biomass on Radar Backscatter from Tree Canopies. *International Journal of Remote Sensing*, 16: 503-513.

Williams R.J., G.A. Duff, D.M.J.S. Bowman and G.D Cook. (1996). Variation in the composition and structure of tropical savannas as a function of rainfall and soil texture along a large-scale climatic gradient in the Northern Territory, Australia. *Journal of Biogeography,* 23: 747-756.

Williams R.J., B.A. Myers, M.J. Muller, G.A. Duff and D. Eamus. (1997). Leaf phenology of woody species in a northern Australian tropical savanna. *Ecology,* 78: 2542-2558.

Yanasse, C. C. F., Sant'Anna, S. J. S., Frery, A. C., Renno, C. D., Soares, J. V., and Zebker , H. A. and van Zyl, J. J., (1991), Imaging Polarimetry: A Review, *Proceedings of the IEEE*, 79: 1583-1606.